BMC Cancer

RESEARCH Open Access

Lenvatinib targets STAT-1 to enhance the M1 polarization of TAMs during hepatocellular carcinoma progression

Peng Sun[1,2], Zhenfeng Li[2], Zaojun Yan[5], Zhaofeng Wang[6], Peng Zheng[7], Mingliang Wang[7], Xu Chang[2], Zihao Liu[2], Jianxin Zhang[2], Huiyong Wu[2], Wenbo Shao[2], Dewen Xue[2] and Jinming Yu[1,3,4*]

Abstract

Lenvatinib, a multitarget kinase inhibitor, has been proven to be effective in the treatment of advanced hepatocellular carcinoma. It has been previously demonstrated that tumour associated macrophages (TAMs) in tumour tissues can promote HCC growth, invasion and metastasis. Furthermore, lenvatinib has certain immunomodulatory effects on the treatment of HCC. However, the role of lenvatinib in macrophage polarization during HCC treatment has not been fully explored. In this study, we used a variety of experimental methods both in vitro and in vivo to investigate the effect of lenvatinib on TAMs during HCC progression. This study is the first to show that lenvatinib can alter macrophage polarization in both humans and mice. Moreover, macrophages treated with lenvatinib in vitro displayed enhanced classically activated macrophages (M1) activity and suppressed liver cancer cell proliferation, invasion, and migration. Furthermore, during the progression of M1 macrophage polarization induced by lenvatinib, STAT-1 was the main target transcription factor, and inhibiting STAT-1 activity reversed the effect of lenvatinib. Overall, the present study provides a theoretical basis for the immunomodulatory function of lenvatinib in the treatment of HCC.

Keywords Lenvatinib, STAT-1, TAMs, HCC

*Correspondence:
Jinming Yu
sdyujinming@163.com
[1]National Clinical Research Center for Cancer, Key Laboratory of Cancer Prevention and Therapy, Tianjin's Clinical Research Center for Cancer, Tianjin Medical University, Tianjin Medical University Cancer Institute and Hospital, Tianjin, China
[2]Department of Intervention Oncology, Shandong Cancer Hospital and Institute, Shandong First Medical University and Shandong Academy of Medical Sciences, Jinan, Shandong, China
[3]Department of Radiation Oncology and Shandong Provincial Key Laboratory of Radiation Oncology, Shandong First Medical University and Shandong Academy of Medical Sciences, Jinan, Shandong, China
[4]Research Unit of Radiation Oncology, Chinese Academy of Medical Sciences, Jinan, Shandong, China
[5]Department of Infection, The People's Hospital of Rizhao, Rizhao, Shandong, China
[6]Surgical Department, Jinan Jiyang District Hospital of Traditional Chinese Medicine, Jinan, Shandong, China
[7]Oncology Department, The People's Hospital of Xiajin, Dezhou, Shandong, China

Introduction

Hepatocellular carcinoma (HCC), which is the most common type of liver cancer, is the fifth most prevalent cancer and the fourth leading cause of death worldwide due to environmental, viral and genetic risk factors [1]. Second only to pancreatic cancer, HCC has an 18% five-year survival rate [2]. Current treatments for HCC include liver transplantation, surgical removal, systemic therapy and liver targeted therapy. Since most HCC patients are diagnosed at an advanced stage because the disease is mostly asymptomatic in the early stages, only 15% of patients have access to surgical treatment [3, 4]. The high recurrence and metastasis rate of HCC after surgery remains a clinical problem. Therefore, it is a major challenge for researchers to identify effective treatment strategies for HCC.

Recent studies have shown that the poor prognosis of HCC patients is closely related to the tumour immune microenvironment. The overall state of the immune microenvironment in HCC tissues is immunosuppressive [5]. Tumour associated macrophages (TAMs) are a group of immune-dysregulated cells in tumour tissues that can promote tumour growth, invasion and metastasis. Due to the diverse functions and strong plasticity of macrophages, current studies have divided them into two main categories: classically activated macrophages (M1) and alternatively activated macrophages (M2) [6, 7]. M1 is mainly controlled by STAT-1, IRF-5 and NF-κB to express numerous pro-inflammatory mediators including TNF-α, IL-6, IL-12 and iNOS [8]. M1 macrophages mainly promote the Th1 immune response, tissue remodelling and bone destruction by secreting these pro-inflammatory mediators, while M2 is mainly regulated by STAT-6, IRF-4 and PPARγ to express molecules including arginase-1, IL-10, and CD206. M2 macrophages have a low antigen presentation ability, promote cellular repair, and enhance tumour actions by secreting anti-inflammatory cytokines [8–10]. It is generally believed that TAMs exhibit the M2 phenotype. TAMs are closely related to the prognosis of patients with HCC [11]. Therefore, changing the immunosuppressive state in HCC tissues and reversing the polarization status of TAMs is the key to HCC treatment.

Table 1 Clinical characteristics of HCC patients

Indicator	HCC patients ($n=8$)
Male, n (%)	6 (75.00)
Age, mean years (range)	54 (38–73)
HBV-DNA, n (+, %)	7 (87.50)
AFP, n (> 100, %)	5 (62.50)
Single tumor, n (%)	4 (50.00)
Lymphatic metastasis, n (%)	3 (37.50)
Distant metastasis, n (%)	2(25.00)

Lenvatinib (LEN) is an oral small molecule multitarget kinase inhibitor for advanced hepatocellular carcinoma that inhibits vascular endothelial growth factor receptor (VEGFR) 1–3, fibroblast growth factor receptor (FGFR) 1–4, and platelet-derived growth factor receptor (PDGFR) [12]. Studies have shown that LEN exerts potent antiangiogenic effects mainly by inhibiting VEGF and FGF signalling in tumour cells [13, 14]. Moreover, studies have shown that LEN has certain immunomodulatory effects. In immunodeficient mice, there is no significant difference in antitumour activity between LEN and sorafenib (a multitarget antitumour drug that inhibits the proliferation of tumour cells mainly by inhibiting RAF/MEK/ERK signalling pathways), but LEN shows stronger antitumour activity in mice with a normal immune system [15]. This study suggested that LEN might also have synergistic effects with immune checkpoint inhibitors. Preliminary clinical trials showed that combination therapy with LEN and pembrolizumab (anti-PD-1 antibody) resulted in an objective remission rate of 46% [16]. In addition, this combination therapy has not only been recognized by the Food and Drug Administration (FDA) as a first-line strategy for treating HCC but has also been used in combination with other immune checkpoint inhibitors [17]. Although it has been reported that VEGF can promote M2 macrophage polarization [18, 19], the direct effects of LEN on TAMs and macrophage polarization remain unknown.

In this study, we found that LEN inhibited M2 macrophage polarization and enhanced M1 macrophage activity both in vitro and in vivo. Moreover, treatment of macrophages with LEN in vitro inhibited the proliferation, invasion, and migration of liver cancer cells. Further studies showed that STAT-1 was the main target transcription factor of LEN induced macrophage polarization. Therefore, the present study provides a theoretical basis for the immunomodulatory function of LEN in the treatment of HCC.

Materials and methods

Human blood sample collection and mononuclear cell separation

Blood samples were initially collected from patients who had been diagnosed with unresectable HCC (Shandong Tumour Hospital, Jinan, Shandong, China), and LEN was determined to be the best treatment for these patients. Blood was collected before and one month after LEN treatment. The blood samples were centrifuged in EZ-SepTM lymphocyte separation tubes (Dakewe, Beijing) for mononuclear cell separation. The research was approved by the medical ethics committee of Shandong Cancer Hospital and Institute, Shandong First Medical University (SDTHEC2022007011). Informed consent

was obtained from the patients. The characteristics of the HCC patients are summarized in Table 1.

Mouse HCC model establishment

C57BL/6 mice were purchased from Weitong Lihua (Beijing). They were kept in a room with a specific temperature and humidity. To establish a mouse HCC model, 100 μl of saline solution containing 1×10^6 H22 cells was subcutaneously injected into the groin of C57BL/6 mice. After 10 days, the mice were randomly divided into two groups according to the tumour size. The mice in the control group were subjected to gavage treatment with 10 mg/kg/day LEN or starch. The tumour size was measured every other day, and the tumour volume was calculated via the $1/2ab^2$ (where a is the long diameter and b is the short diameter) formula. The mice were anaesthetized with pentobarbital sodium (50 mg/kg, i.p.). All the mouse experiments were approved by the Animal Care Committee of Shandong Cancer Hospital and Institute, Shandong First Medical University (SDTHEC202201044), and were performed according to the Animal Management Rules of the Chinese Ministry of Health.

Macrophage culture and polarization induction

Human macrophages induced from THP-1 cells by PMA (50 nM) were cultured in RPMI-1640 supplemented with 10% foetal bovine serum (FBS). The TAM status was similar to that of M2 macrophage polarization induced by human IL-4 (20 ng/mL) and human IL-13 (20 ng/mL). Mouse peripheral macrophages (PMs) and bone marrow-derived macrophages (BMDMs) were cultured in Dulbecco's modified Eagle's medium (DMEM) supplemented with 10% foetal bovine serum (FBS). M2 macrophage polarization was induced by murine IL-4 (20 ng/mL). For the LEN stimulation assay, LEN was added to the cells 24 h after IL-4 and/or IL-13 was added. For the fludarabine inhibition assay, fludarabine (5 μM) was added to the cells 12 h earlier than LEN.

Flow cytometry (FCM)

FCM was used to detect the surface marker expression level during macrophage polarization. Human peripheral blood mononuclear cells were stained with anti-human CD14-APC (BioLegend, USA) and anti-human CD86-FITC (BioLegend, USA) antibodies or with anti-human CD14-FITC (BioLegend, USA), anti-human CD206-PE-Cy-7 (BioLegend, USA) and anti-human CD163-PE (BioLegend, USA) antibodies for 30 min. The status of macrophages in the tumour tissues was analysed by FCM directly after digestion, grinding and density gradient separation. The macrophages were stained with anti-mouse CD11b-FITC (BioLegend, USA), anti-mouse CD206-PE-Cy-7 (BioLegend, USA), anti-mouse CD86-PE (BioLegend, USA) and anti-mouse PD-L1-APC (BioLegend, USA) antibodies. The antitumour activity of CD8+T cells was analysed by FCM after stimulation with PMA (50 ng/mL) and ionomycin (1 μg/mL) for 6 h and blocking with BFA (10 μg/mL) for 4 h. Then, the CD8+T cells were stained with anti-mouse CD8-PerCP-Cy5.5 (BioLegend, USA), anti-mouse TNF-α-PE-Cy-7 (BioLegend, USA), anti-mouse IFN-γ-BV421 (BioLegend, USA) and anti-mouse CD107a-PE (BioLegend, USA) antibodies. To determine the polarization status of the macrophages, human macrophages, PMs and BMDMs were stained with the corresponding CD86-APC (BioLegend, USA), CD206-FITC (BioLegend, USA) and PD-L1-APC (BioLegend, USA) antibodies. At least 10,000 cells were analysed with a BD FACSAria II. The cells were gated by their forwards and side scatter properties.

Ki67 staining

10 Formaldehyde-fixed paraffin sections collected from mice HCC model were incubated with Ki67 (CST, 1:200) overnight at 4 °C. As a negative control, species- and isotype-matched IgG were applied in place of the primary antibody. Immunoreactivity was visualized after incubation with the appropriate horseradish peroxidase-conjugated secondary antibodies. The slides were viewed in 400× magnification with a microscope (BX41, Olympus) and with a digital camera (Spot Insight 2, Diagnostic Instruments, Inc.).

HCC cell culture

The human HCC cell line HepG2 (American Type Culture Collection), mouse HCC cell line H22 (American Type Culture Collection) and Hepa1-6 (American Type Culture Collection) were cultured in DMEM supplemented with 10% foetal bovine serum (FBS).

Real-time PCR

According to the manufacturer's protocol, RNA was extracted from human macrophages, PMs and BMDMs using a Fast Gene RNA isolation kit (cat. no. 220011). cDNA was subsequently generated with a Takara reverse transcription kit (cat. no. RR037A). The PCR thermocycling conditions (Bio-Rad Laboratories, Inc.) were as follows: 95 °C for 30 s, followed by 40 cycles of 95 °C for 5 s. The related primer sequences for PCR are listed in Table 2.

Western blot

Total proteins were extracted from macrophages. Proteins were separated by 10% SDS–PAGE and then transferred to PVDF membranes. After the membranes were blocked with 5% bovine serum albumin for 2 h at room temperature, they were incubated with specific primary antibodies (anti-phospho-STAT-1, anti-STAT-1, anti-phospho-STAT-6, anti-STAT-6, or anti-β-actin) at 4 °C

Table 2 The sequence of the primer for RT-PCR

Primer	Sequence
Homo-β-actin	Forward: CATGTACGTTGCTATCCAGGC
	Reverse: CTCCTTAATGTCACGCACGAT
Homo-arginase-1	Forward: TGACGGACTGGACCCATCTT
	Reverse: GGCTTGTGATTACCCTCCCG
Homo-IL-10	Forward: CCAGACATCAAGGCGCATGT
	Reverse: GATGCCTTTCTCTTGGAGCTTATT
Homo-TGF-β	Forward: GCAACAATTCCTGGCGATACC
	Reverse: ATTTCCCCTCCACGGCTCAA
Homo-IL-6	Forward: CCTGAACCTTCCAAAGATGGC
	Reverse: TTCACCAGGCAAGTCTCCTCA
Homo-IL-1β	Forward: AGCTGGAGAGTGTAGATCCCAA
	Reverse: ACGGGCATGTTTTCTGCTTG
Mouse-b-actin	Forward: CCACACCCGCCACCAGTTCG
	Reverse: TACAGCCCGGGGAGCATCGT
Mouse-arginase-1	Forward: TGTCCCTAATGACAGCTCCTT
	Reverse: GCATCCACCCAAATGACACAT
Mouse-IL-10	Forward: GGACAACATACTGCTAACCGACTC
	Reverse: CCTGGGGCATCACTTCTACC
Mouse-TGF-β	Forward: ACCGCAACAACGCCATCTAT
	Reverse: TGCCGTACAACTCCAGTGAC
Mouse-IL-6	Forward: ACAACCACGGCCTTCCCTAC
	Reverse: CATTTCCACGATTTCCCAGA
Mouse-IL-1β	Forward: ACCTTCCAGGATGAGGACATGA
	Reverse: AACGTCACACACCAGCAGGTTA

overnight. After washing three times and incubation with specific conjugated peroxidase-labelled secondary antibodies, the immunoreactive bands were visualized by using chemiluminescence (ECL) reagents. A Western blot imaging system (GE, Amersham Imager 680) was used to detect protein bands and obtain images.

Migration, invasion and growth of the tumour cells

Culture supernatants from the corresponding macrophages (after the removal of IL-4, LEN, or fludarabine, macrophages were cultured in complete medium for another 12 h to collected the supernatants) were used to culture HepG2 cells and Hepa1-6 cells. The medium for the tumour cells in these assays is a mixture of corresponding macrophages supernatants and complete medium in a ratio of 1:1. Standard Transwell (Corning, 3422) assays were used to measure the migration and invasion of tumour cells (the mixture supernatants was added into the lower chamber). For the colony formation assay, 500 liver cancer cells were plated in six-well plates before the mixture supernatants were added. A 0.1% crystal violet solution was added to the wells for cell staining after methanol treatment.

Statistical analysis

All the data were analysed by GraphPad Prism 8 (GraphPad Software Inc., San Diego, CA, USA). The normality test was performed first, and then Student's t test was used to determine differences between groups. The data are reported as the means±SEMs. A p value <0.05 was considered to indicate a significant difference. $^{*}p<0.05$, $^{**}p<0.01$, $^{***}p<0.001$, ns indicates no significance.

Results

LEN modulates the polarization of monocytes in HCC patients

Since LEN is a first-line drug for the treatment of HCC, the primary task of this study was to determine the effect of LEN on monocyte polarization in HCC patients. We collected monocytes from HCC patients before and after the administration of LEN. CD86, CD206, and CD163 were detected by flow cytometry (FCM). CD86 on monocytes (labelled with CD14), which is a marker of M1 macrophages, was downregulated after the administration of LEN (Fig. 1A). The expression of CD206 and CD163, which are markers of M2 macrophages, was also reduced after the administration of LEN (Fig. 1B and C). We conclude that LEN has the effect on the monocytes in HCC patients from these results.

LEN modulates the polarization of macrophages in a mouse HCC model

Because LEN can alter monocyte polarization in HCC patients, we established a mouse HCC model with H22 cells. Compared with the control group (starch), the LEN group exhibited significant tumour suppressive activity. The results showed that LEN inhibited the growth of the HCC model (Fig. 2A and B). The tumour weight of the LEN group was significantly lower than that of the control group (control, 1.08 g±0.24 g; LEN, 0.36 g±0.17 g) (Fig. 2C and E). Furthermore, Ki67 staining, which is a marker of tumour proliferation, showed that LEN inhibited the proliferation of HCC cells (Fig. 2F).

Further analysis of infiltrating macrophages (labelled with CD11b) in the tumour tissues revealed that LEN could enhance the expression of the M1 marker CD86 (Fig. 3A) and reduce the expression of the M2 markers CD206 (Fig. 3B) and PD-L1 (Fig. 3C). These results indicated that LEN promoted the M1 polarization of TAMs and suppressed their M2 polarization. Since there is evidence that LEN can activate the antitumour activity of CD8+T cells when combined with an anti-PD-1 antibody [20], markers of antitumour activity for CD8+T cells in corresponding tumour tissues were also detected by FCM. As shown in Fig. 3D and F, LEN increased the expression of TNF-α, IFN-γ, and CD107a, which reflects the antitumour activity of CD8+T cells [21]. This result is consistent with those of previous studies.

LEN modulates the polarization of macrophages in vitro

The above results indicated that LEN could affect the polarization of macrophages in vivo. Then, we cultured

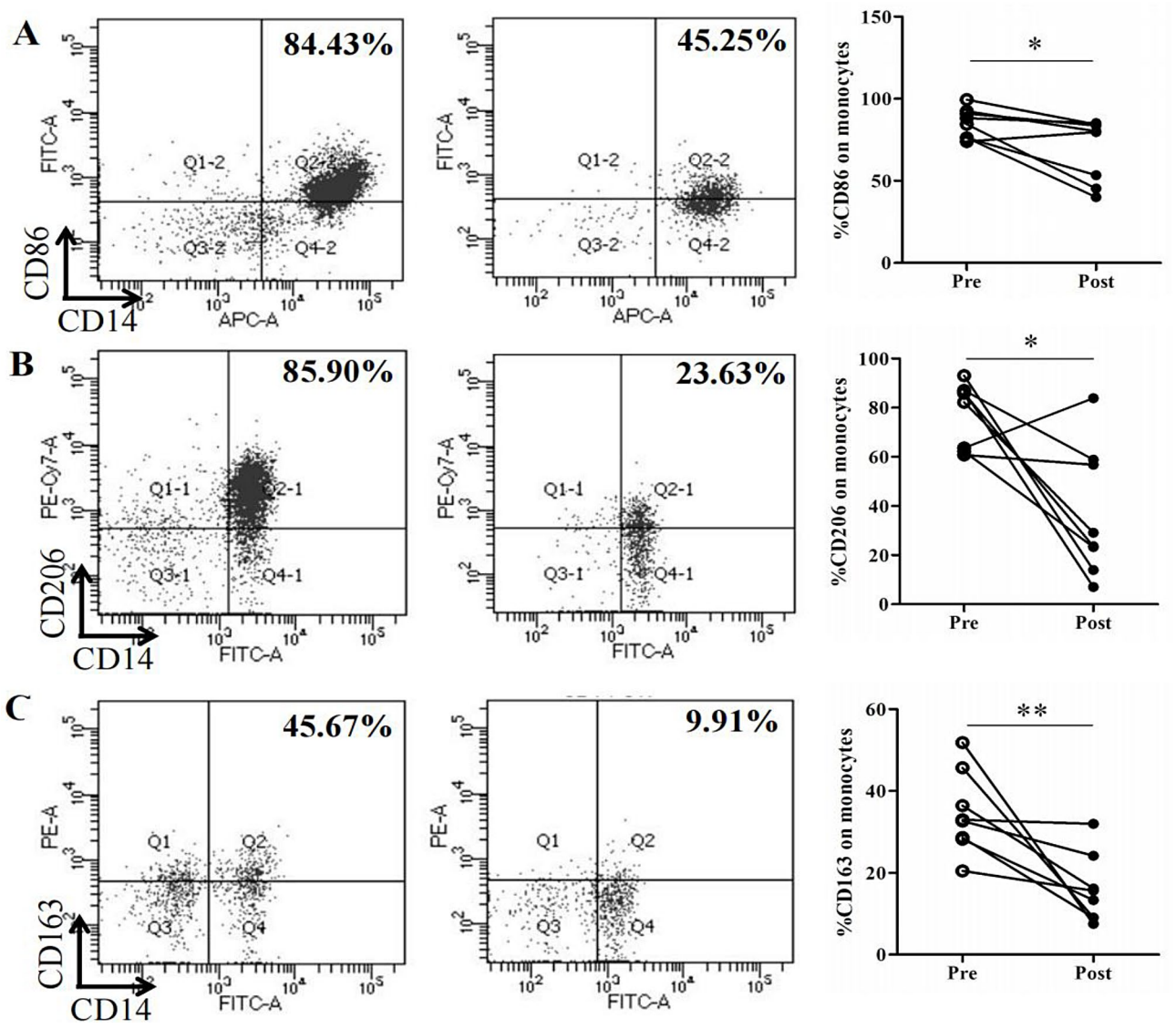

Fig. 1 The polarization state of monocytes in HCC patients. We collected monocytes from the peripheral blood of HCC patients before and after the administration of LEN ($n=8$). CD86, CD206, and CD163 on monocytes labelled with CD14 were detected by flow cytometry (FCM). A representative graph is shown on the left, and a statistical graph is shown on the right. (**A**) The percentage of CD86 + CD14 + monocytes was determined by FCM before (85.21%±3.25%) and after (68.98%±6.81%) LEN treatment. (**B**) The percentage of CD206 + CD14 + monocytes was determined by FCM before (77.67%±4.66%) and after (37.08%±9.38%) LEN treatment. (**C**) The percentage of CD163 + CD14 + monocytes was determined by FCM before (34.61%±3.55%) and after (15.87%±2.98%) LEN treatment. The data are presented as the means ± SEMs. *$p<0.05$, **$p<0.01$

three kinds of macrophages (human macrophages derived from THP-1 cells, mouse peritoneal macrophages (PMs), and mouse bone marrow-derived macrophages (BMDMs)) to test the effect of LEN on the polarization of macrophages in vitro. As shown in Fig. 4A, the real-time PCR results revealed that arginase-1 (arg-1), interleukin-10 (IL-10), and transforming growth factor-β (TGF-β) in human macrophages were downregulated after LEN treatment. These indicators are highly expressed in M2 macrophages. However, the expression of IL-6 and IL-1β, which are highly expressed in M1 macrophages, tended to increase, although this difference was not significant. The results for PMs (Fig. 4B) and BMDMs (Fig. 4C) treated with LEN were in accordance with those for human macrophages. Then we detected the level of these cytokines in the macrophages supernatants by ELISA. The expression level of IL-10, TGF-β and IL-6 in supernatants was consistent with RNA expression (Fig. 4D and E).

The expression of CD206, CD86 and PD-L1 on the corresponding macrophages was also analysed by FCM. The results showed that LEN inhibited the expression of CD206 in human macrophages compared with that in the control group. However, there was no significant

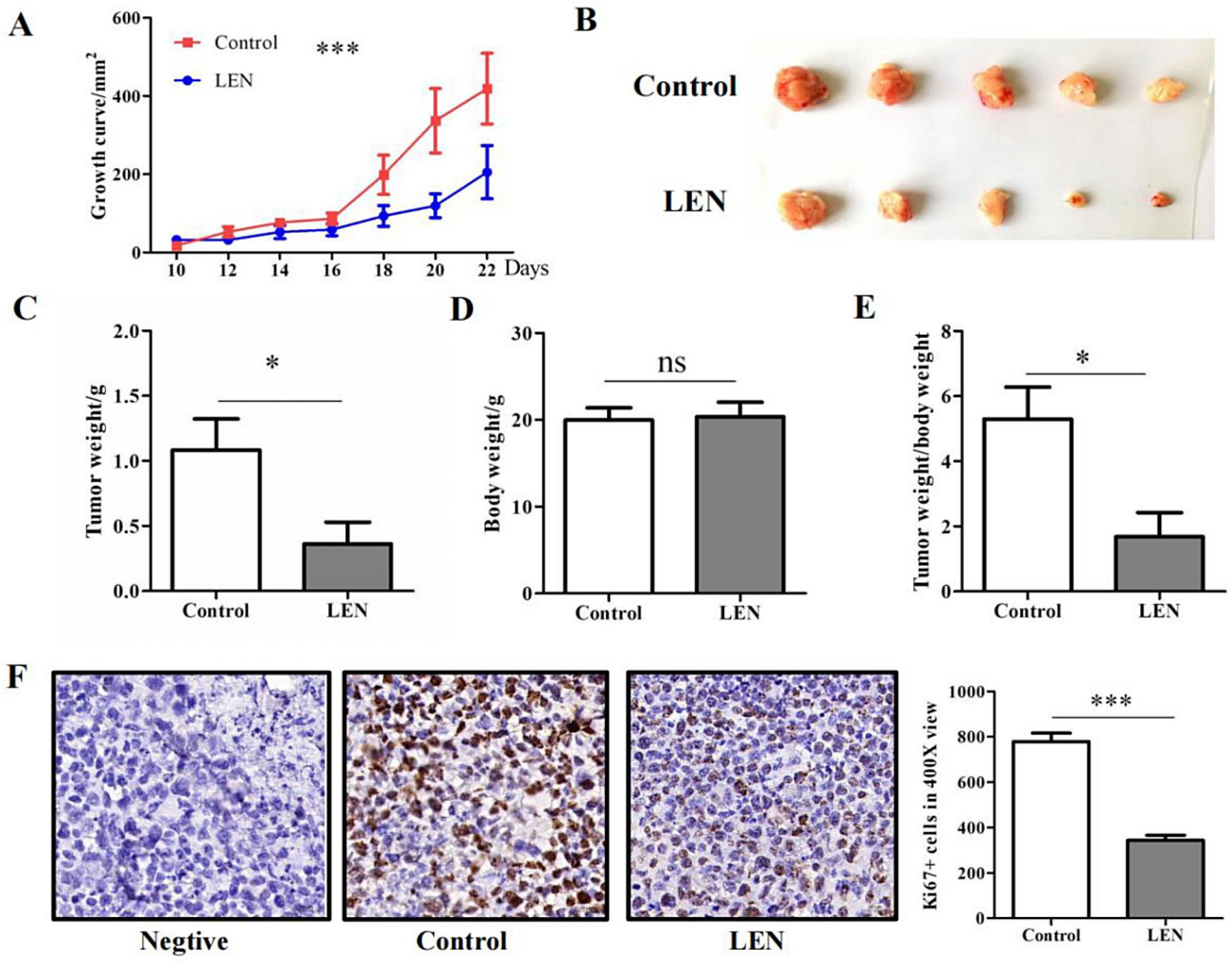

Fig. 2 The effect of LEN on HCC growth. A mouse HCC model ($n = 5$) was established with H22 cells, a mouse hepatocellular carcinoma cell line. Then, the mice were given LEN (10 mg/kg/day) or control starch by gavage every day for 10 days. (**A**) The tumour growth curve, which was measured via tumour size, is shown. (**B**) The tumour images of the two groups are presented at the time of sacrifice. (**C**) The tumour weights of the two groups were measured (control, 1.08 g ± 0.24 g; LEN, 0.36 g ± 0.17 g). (**D**) The body weights of the two groups were measured (control, 19.99 g ± 1.41 g; LEN, 20.36 g ± 1.68 g). (**E**) The ratio of tumour weight to body weight is presented (control, 5.29 ± 0.98; LEN, 1.68 ± 0.74). (**F**) Immunohistochemical staining for Ki67 was performed to evaluate the proliferation of HCC cells. A typical graph is shown on the left, and a statistical graph is shown on the right. (Control, 778.80 ± 37.80; LEN, 343.80 ± 22.46). The data are presented as the means ± SEMs. *$p < 0.05$, ***$p < 0.001$, ns indicates no significance

difference in CD86 and PD-L1 expression between the two groups (Fig. 5A). LEN downregulated the expression of CD206, PD-L1 and upregulated the expression of CD86 in PMs and BMDMs (Fig. 5B and C). All these results indicated that LEN could inhibit M2 macrophage polarization and enhance M1 macrophage activity in vitro.

LEN inhibits the progression of hepatocellular carcinoma by affecting macrophage polarization

To determine whether LEN could inhibit the progression of hepatocellular carcinoma through macrophages, we collected the supernatants of the corresponding macrophages that were treated with or without LEN to coculture liver cancer cells (human macrophages to HepG2 cells; PMs and BMDMs to Hepa1-6 cells). Because migration, invasion and colony formation assays can reflect the progression of liver cancer cells, we used these three experiments to demonstrate the role of macrophages. As shown in Fig. 6A, the supernatants of human macrophages treated with LEN suppressed the migration (left) and invasion (right) of HepG2 cells. The supernatants from the PMs (Fig. 6B) and BMDMs (Fig. 6C) showed the same results as those from the human macrophages.

Then, the supernatants from the corresponding macrophages were used for the colony formation assay. Compared with those of the control group, the LEN-treated human macrophage supernatants inhibited the growth of HepG2 cells (Fig. 7A). In addition, the number of colonies formed by Hepa1-6 cells cocultured with the

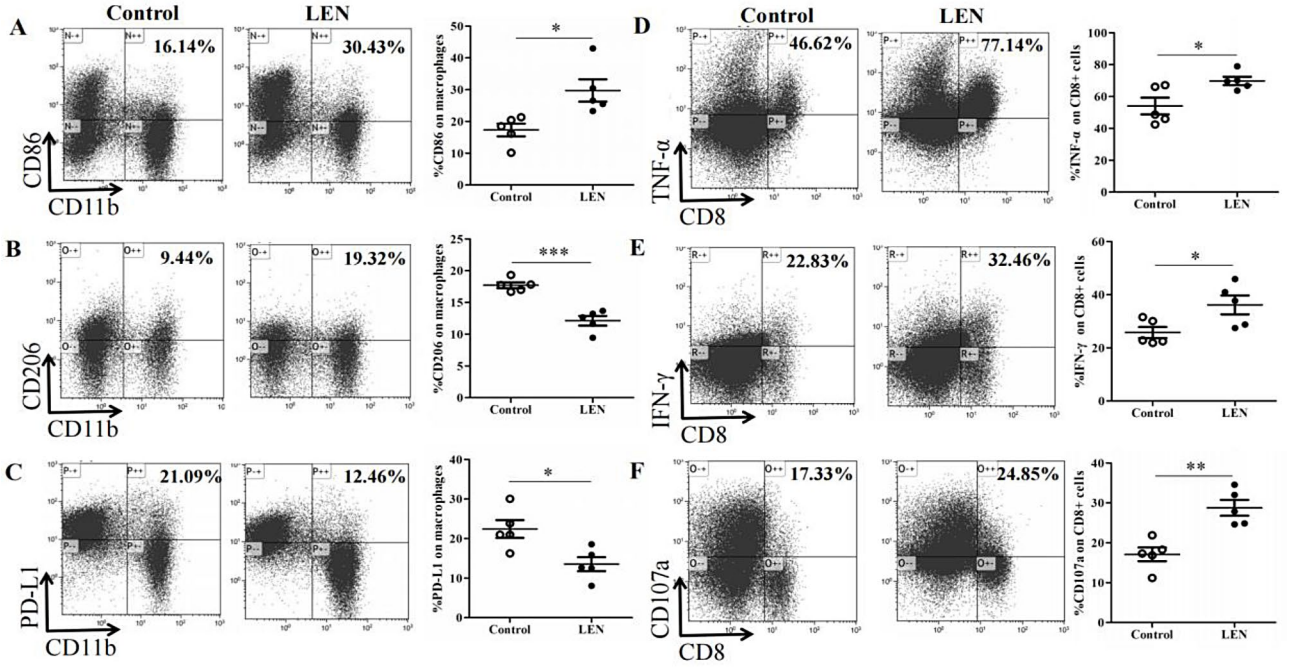

Fig. 3 The status of macrophages and CD8 + T cells in the tumour microenvironment. The tumour tissues collected from the mice at the time of sacrifice are presented in Fig. 2B. The tumour tissues from the control and LEN groups were digested, ground and separated to obtain immune cells. FCM analysis was performed to detect the status of macrophages and CD8 + T cells. Typical images are presented in the left panel, while summary data are presented in the right panel. (**A**) The percentage of CD86 + macrophages labelled with CD11b is shown (control, 17.31%±2.00%; LEN, 29.75%±3.51%). (**B**) The percentage of CD206 + macrophages is shown (control, 17.71%±0.46%; LEN, 12.13%±0.75%). (**C**) The percentage of PD-L1 + macrophages is shown (control, 22.41%±2.26%; LEN, 13.52%±1.77%). The antitumour activity of CD8 + T cells was analysed by FCM after stimulation with PMA (50 ng/mL) and ionomycin (1 μg/mL) and blocking with BFA (10 μg/mL). (**D**) The percentage of TNF-α-positive CD8 + T cells labelled with CD3 + CD8 + cells is shown (control, 54.05%±5.24%; LEN, 69.80%±2.55%). (**E**) The percentage of IFN-γ + CD8 + T cells is shown (control, 25.76%±2.08%; LEN, 36.17%±3.54%). (**F**) The percentage of CD107a + CD8 + T cells is shown (control, 17.10%±1.72%; LEN, 28.77%±1.97%). The data are presented as the means ± SEMs. *$p < 0.05$, **$p < 0.01$, ***$p < 0.001$

supernatants from PMs (Fig. 7B) and BMDMs (Fig. 7C) treated with LEN was much lower than that formed by the control group. LEN not only directly inhibited the progression of hepatocellular carcinoma, as described in previous studies [12–14], but also indirectly affected hepatocellular carcinoma progression by modulating macrophage polarization.

LEN modulates M1 macrophage polarization by increasing the phosphorylation of STAT-1

Through the above studies, we found that LEN could inhibit the progression of hepatocellular carcinoma by regulating the polarization of macrophages both in vivo and in vitro. To explore the mechanisms involved in this progression, we detected the phosphorylation levels of polarization-related transcription factors in macrophages. Since signal transducer and activator of transcription-1 (STAT-1) and STAT-6 are the key transcription factors involved in macrophage polarization [22], the phosphorylation levels of STAT-1 and STAT-6 in these macrophages were analysed by western blotting. As shown in Fig. 7D, p-STAT-1 in human macrophages was upregulated after treatment with LEN, whereas there was no difference in p-STAT-6 between these two groups. Moreover, the results for PMs (Fig. 7E) and BMDMs (Fig. 7F) were consistent with those for human macrophages. These results suggested that LEN intervention could promote the phosphorylation of STAT-1 during macrophage polarization.

To demonstrate that p-STAT-1 is the key target in LEN-induced M1 macrophage polarization, we used the STAT-1 activation inhibitor fludarabine [23] in subsequent experiments. LEN did not affect the level of p-STAT-1 in PMs that were pretreated with fludarabine (Fig. 8A). Based on the results of PCR (Fig. 8B), ELISA (Fig. 8C) and FCM (Fig. 8D), pretreatment with fludarabine clearly reversed the effect of LEN on macrophage polarization. The migration (Fig. 8E), invasion (Fig. 8F), and colony formation (Fig. 8G) abilities of the supernatants collected from the macrophages pretreated with fludarabine followed by LEN were the same as those of the Hepa1-6 cells. This result indicated that STAT-1 is the key transcription factor involved in the M1 macrophage polarization induced by LEN.

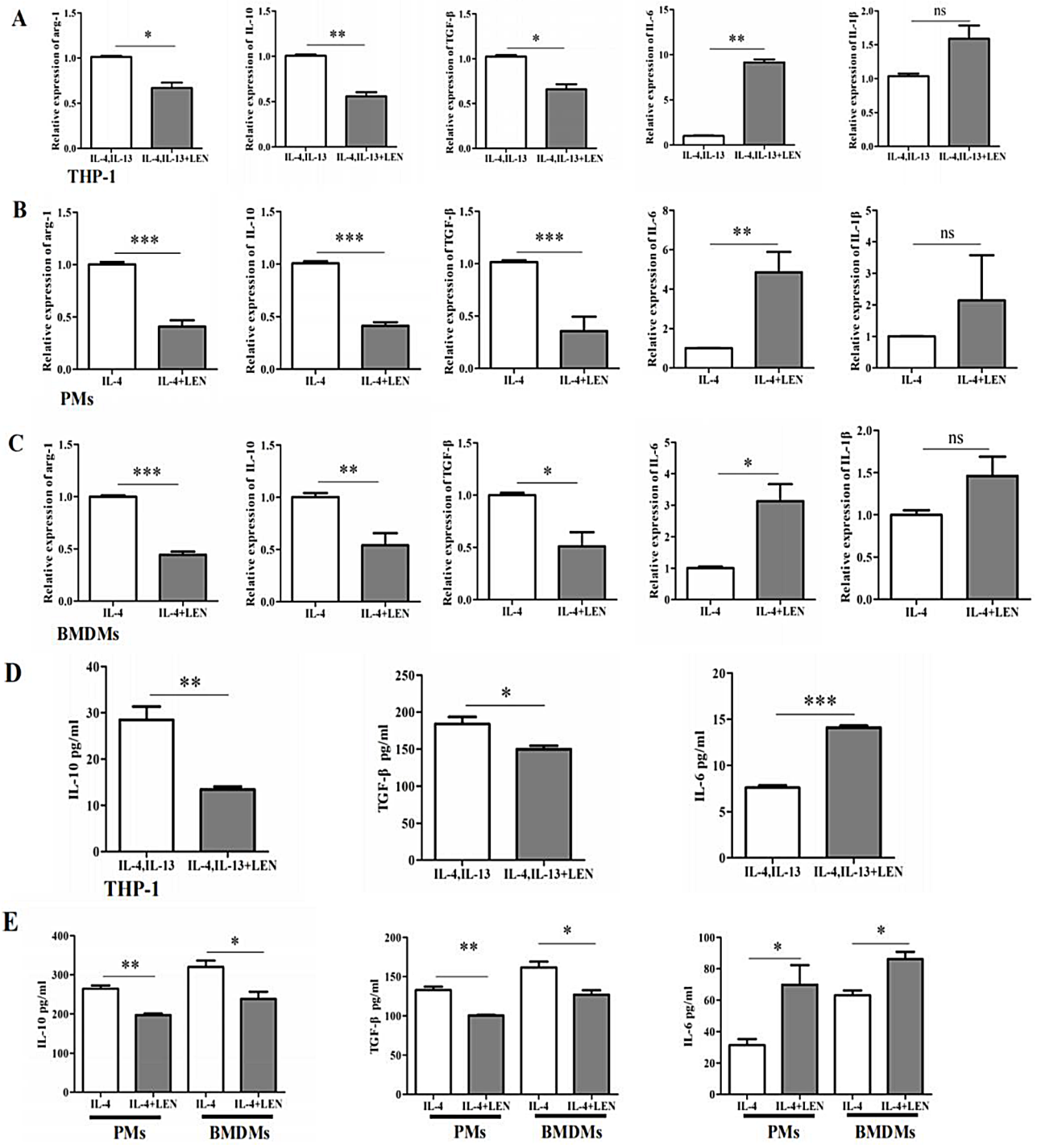

Fig. 4 M1 macrophage polarization induced by LEN was confirmed. The THP-1, PMs, BMDMs were induced to M2 cells and then treated with LEN. Reverse transcription-quantitative PCR was performed to determine the relative expression of arginase-1, IL-10, TGF-β, IL-6, and IL-1β. (**A**) The expression of arginase-1, IL-10, TGF-β, IL-6, and IL-1β in THP-1 treated with or without LEN was analysed by RT–PCR. (**B**) The expression of arginase-1, IL-10, TGF-β, IL-6, and IL-1β in PMs treated with or without LEN was analysed by RT–PCR. (**C**) The expression of arginase-1, IL-10, TGF-β, IL-6, and IL-1β in BMDMs treated with or without LEN was analysed by RT–PCR. Then the level of IL-10, TGF-β, IL-6 in these cell supernatants were also detected by ELISA. (**D**) The IL-10, TGF-β, IL-6 from THP-1 cells treated with or without LEN was detected by ELISA. (**E**) The IL-10, TGF-β, IL-6 from PMs treated with or without LEN were detected by ELISA. (**F**) The IL-10, TGF-β, IL-6 from BMDMs treated with or without LEN were detected by ELISA. Data are presented as the means ± SEMs. *$p < 0.05$, **$p < 0.01$, ***$p < 0.001$, ns indicates no significance

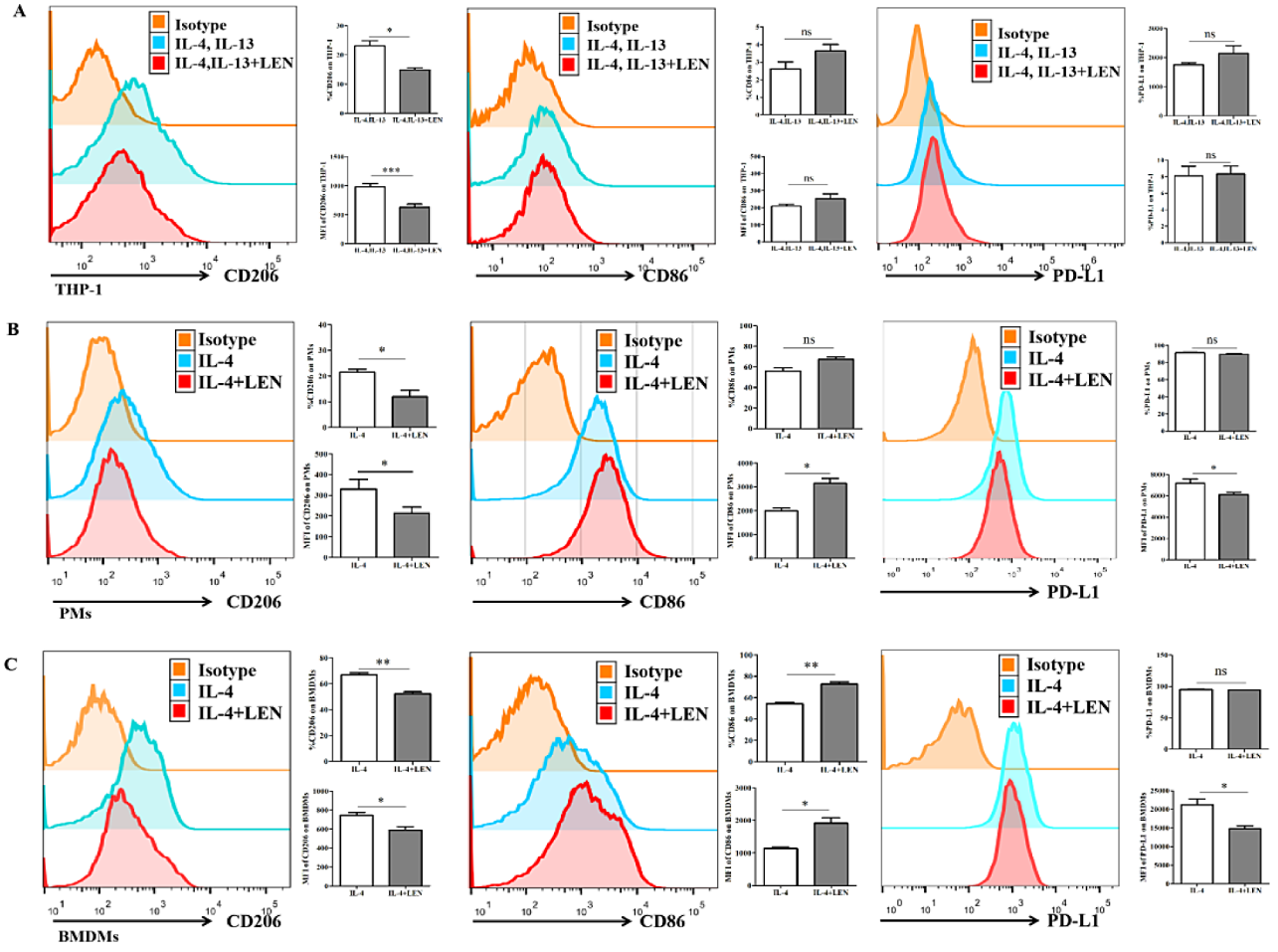

Fig. 5 M1 macrophage polarization induced by LEN detected by FCM. The expression of CD206, CD86 and PD-L1 on the corresponding macrophages was detected by FCM. Typical images are presented in the left panel, while summary data for the percentage (up) and mean fluorescence intensity (down) are presented in the right panel. (**A**) CD206, CD86 and PD-L1 expression on human macrophages treated with or without LEN was analysed by FCM. (**B**) CD206, CD86 and PD-L1 expression on PMs treated with or without LEN was analysed by FCM. (**C**) CD206, CD86 and PD-L1 expression on BMDMs treated with or without LEN was analysed by FCM. The data are presented as the means ± SEMs. *$p < 0.05$, **$p < 0.01$, ***$p < 0.001$, ns indicates no significance

Discussion

As a multitargeted tyrosine kinase inhibitor (TKI), LEN controls the progression of HCC by directly inhibiting VEGFR, FGFR, PDGFR, etc., on tumour cells [12]. This conclusion was verified by our results, which showed that mice orally administered LEN had a much slower progression of HCC than control mice (Fig. 2). It has also been reported that LEN can restrain HCC progression by indirectly regulating the function of various immune cells. Past studies have reported that when combined with PD-1 blockade, LEN can modulate cancer immunity in the tumour microenvironment by reducing TAMs [20] and increasing CD8+T-cell populations [15]. Moreover, FGFR inhibition with LEN enhances antitumour immunity and the activity of anti-PD-1 antibodies [24]. In addition, the combination of LEN with an anti-Gr-1 antibody ameliorated the expansion of myeloid-derived suppressor cells (MDSCs) by LEN and significantly improved the antitumour effect of LEN [25]. In this study, we found that the application of LEN could alter the polarization status of mono-macrophages in both humans and mice (Figs. 1 and 3). In addition, the result of CD8+T cells in the tumour environment was consistent with a previous report [15]. Interestingly, CD86, which is a marker of M1 polarization, was downregulated after LEN treatment in HCC patients. This result, contrary to other results, needs further investigation.

In recent years, increasing attention has been given to the functions of TAMs during the progression of HCC. TAMs are mostly polarized towards the M2 phenotype in the HCC tumour microenvironment and promote HCC growth, angiogenesis, invasion and metastasis [26]. CD68 and CD14 have been used as biological markers for TAMs, which are key players in cancer-related inflammation in HCC tissues [27, 28]. Moreover, there is a clear correlation between the number of TAMs and the

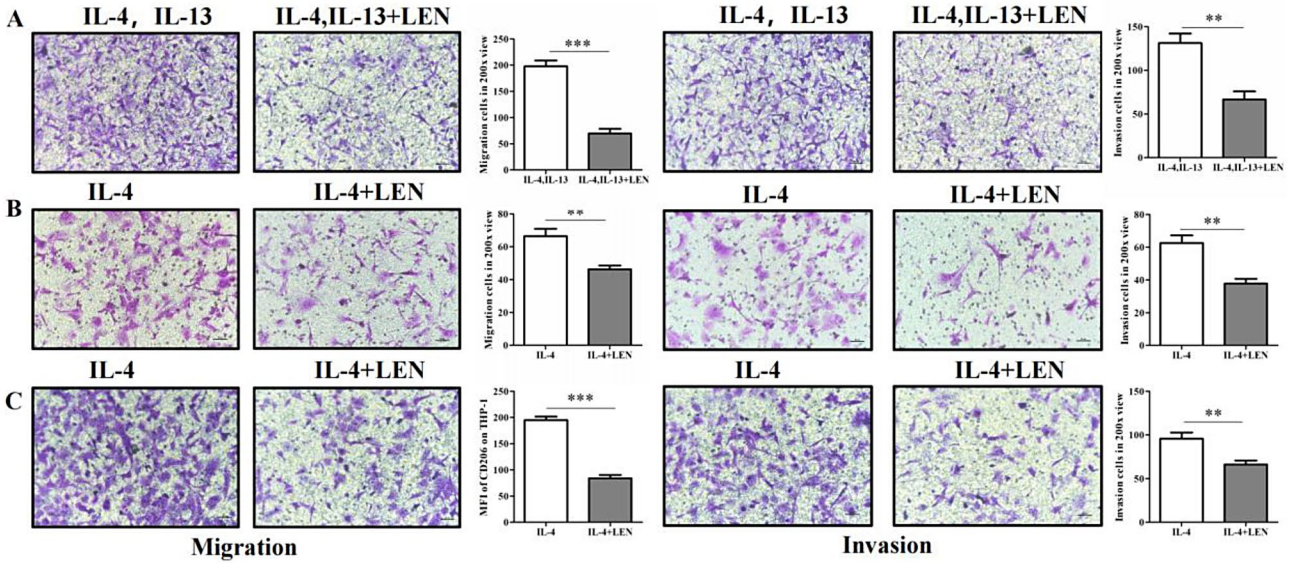

Fig. 6 The effect of macrophages induced by LEN on the migration and invasion of HCC cells. The supernatants of corresponding macrophages treated with or without LEN were collected for migration and invasion assays. A typical graph is shown on the left, and a statistical graph is shown on the right. (**A**) The migration and invasion of HepG2 cells cocultured with the supernatants of THP-1 are shown. (**B**) The migration and invasion of Hepa1-6 cells cocultured with the supernatants of PMs are shown. (**C**) The migration and invasion of Hepa1-6 cells cocultured with the supernatants of BMDMs are shown. The data are presented as the means ± SEMs. $^{**}p < 0.01$, $^{***}p < 0.001$

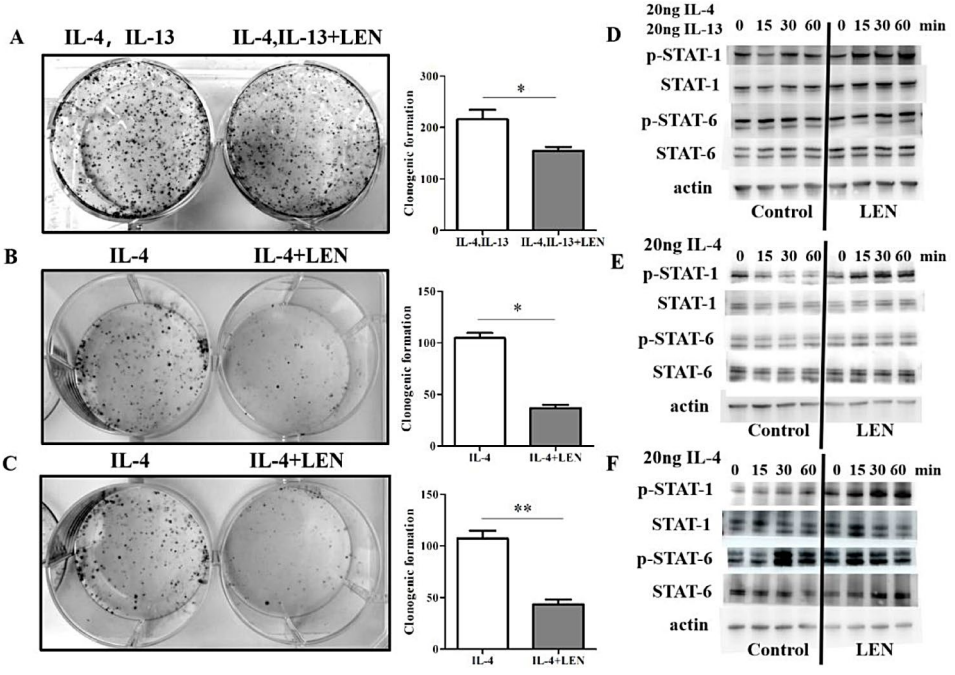

Fig. 7 The effect of macrophages induced by LEN on the growth of HCC cells. The supernatants of the corresponding macrophages treated with or without LEN were collected for the colony formation assay. A typical graph is shown on the left, and a statistical graph is shown on the right. (**A**) The growth of HepG2 cells cocultured with the supernatants of THP-1 is shown. (**B**) The growth of Hepa1-6 cells cocultured with the supernatants of PMs is shown. (**C**) The growth of Hepa1-6 cells cocultured with the supernatants of BMDMs is shown. LEN affected macrophage polarization via STAT-1. The levels of p-STAT-1, STAT-1, p-STAT-6, and STAT-6 were explored by Western blotting (control on the left and LEN on the right). (**D**) The expression of p-STAT-1, STAT-1, p-STAT-6, and STAT-6 in THP-1 was evaluated by Western blotting. (**E**) The expression of p-STAT-1, STAT-1, p-STAT-6, and STAT-6 in PMs was evaluated by Western blotting. (**F**) The expression of p-STAT-1, STAT-1, p-STAT-6, and STAT-6 in BMDMs was evaluated by Western blotting. The data are presented as the means ± SEMs. $^{*}p < 0.05$, $^{**}p < 0.01$

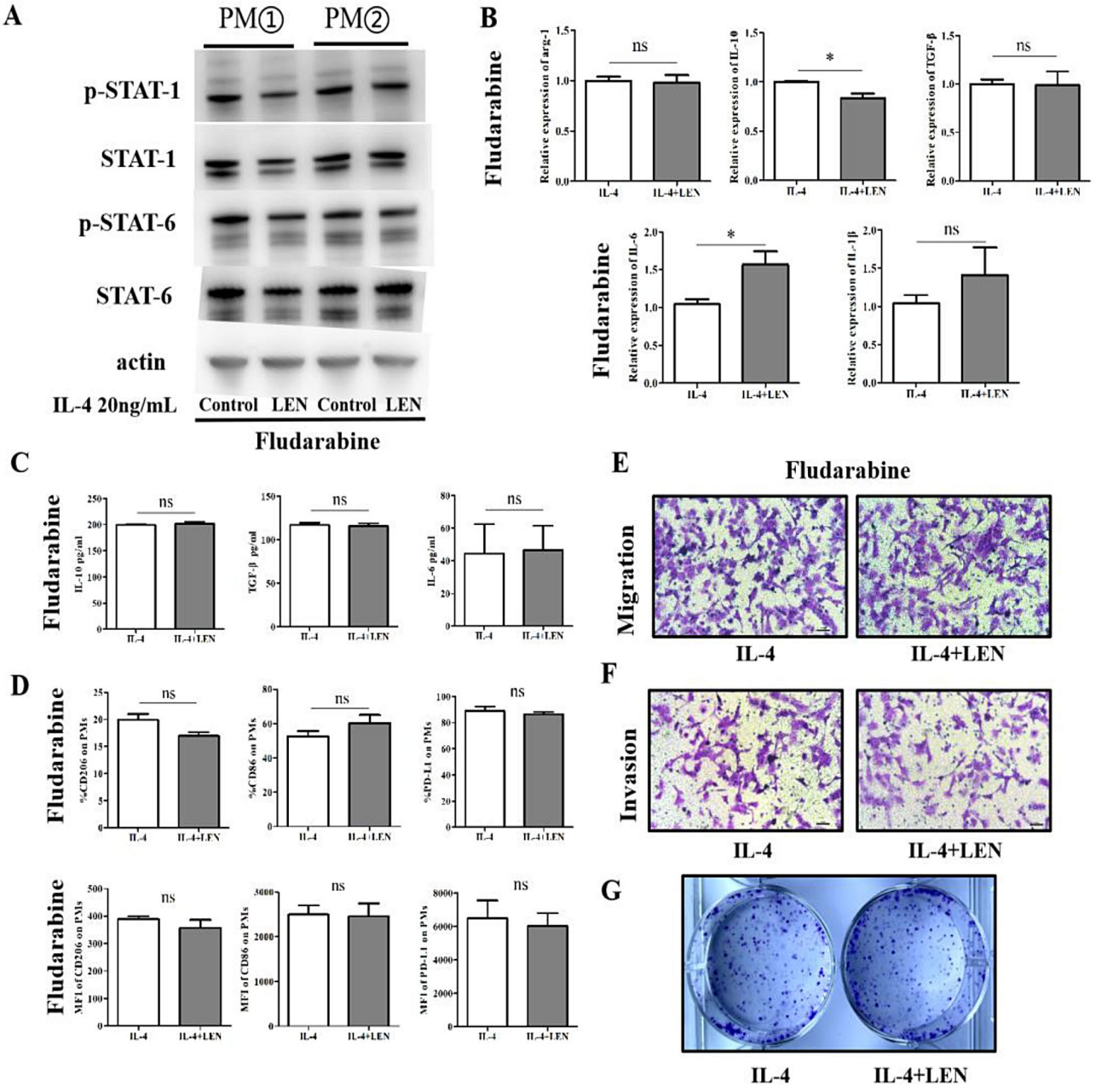

Fig. 8 Fludarabine reversed the M1 macrophage polarization induced by LEN. PMs that were pretreated with fludarabine and then LEN were prepared for subsequent experiments. (**A**) The levels of p-STAT-1, STAT-1, p-STAT-6, and STAT-6 were explored by Western blotting. (**B**) The expression of arginase-1, IL-10, TGF-β, IL-6, and IL-1β on PMs was analysed by RT–PCR. (**C**) The level of IL-10, TGF-β, IL-6 from the supernatants of PMs above was detected by ELISA. (**D**) CD206, CD86 and PD-L1 expression on PMs was analysed by FCM. The summary data for the percentage (up) and mean fluorescence intensity (down) are presented. (**E**) Hepa1-6 cells were cocultured with the supernatants of PMs for the migration assay. (**F**) Hepa1-6 cells were cocultured with the supernatants of PMs for invasion assays. (**G**) Hepa1-6 cells were cocultured with the supernatants of PMs for the colony formation assay. The data are presented as the means ± SEMs. *$p < 0.05$, ns indicates no significance

progression of HCC [29]. On the one hand, TAMs suppress the antitumour immune response by interacting with other immune cells in the tumour microenvironment. On the other hand, TAMs can act upon tumour cells directly by releasing cytokines such as IL-6 and TGF-β, which favour tumour growth, and TNF-α, osteopontin, and matrix metalloproteases (MMPs), which support tumour invasion and metastasis [28]. In the present study, we found that LEN inhibited the expression of M2 markers, including arginase-1, IL-10, TGF-β, and CD206, and promoted the expression of M1 markers, such as IL-6, IL-1β, and CD86 (Figs. 4 and 5). These results indicated that LEN could alter macrophage polarization. Moreover, the supernatants of macrophages

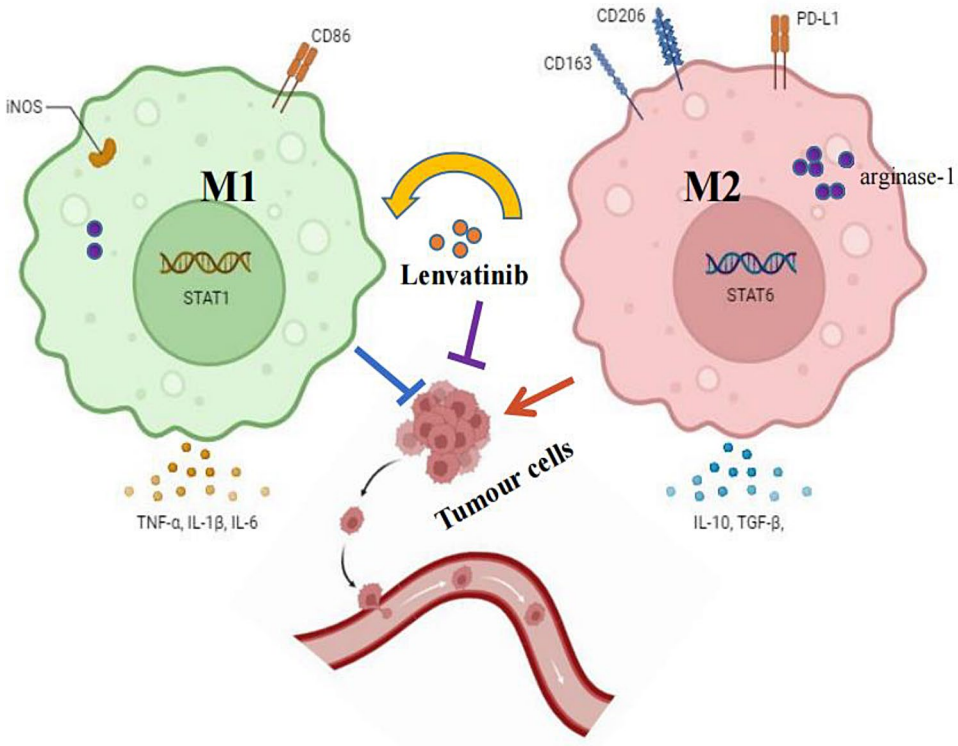

Fig. 9 LEN targets STAT-1 to enhance the M1 polarization of TAMs. On one hand, LEN could inhibit the tumour progression via acting directly on tumour cells. On the other hand, the LEN restrain tumour progression via enhancing TAMs M1 polarization (more CD86, IL-6, IL-1β) and inhibiting M2 polarization (less CD206, PD-L1, IL-10, TGF-β) through STAT-1

treated with LEN displayed inhibitory effects on HCC cells (Figs. 6 and 7). Since it is unclear whether M1 or M2 macrophages express high levels of IL-6, we detected increased IL-6 expression after treatment with LEN.

Due to the control of various transcription factors, different phenotypes of macrophages are generated. Previous reports have demonstrated that C/EBP-α, C/EBP-δ, IRF-9, STAT-1, KLF-6, and NF-κB are key transcription factors that function in M1 macrophage polarization; while C/EBP-β, PPARs, STAT-3, STAT-6 and KLF-4 play a role in M2 macrophage polarization [30–32]. TAMs often have the same transcript profile as M2 macrophages [33]. On the one hand, in the presence of IFN-γ derived mostly from the Th1 response, STAT-1 is a vital mediator of M1 macrophage polarization. On the other hand, in the presence of IL-4 and/or IL-13 derived from the Th2 response, STAT-6 is required to activate M2 macrophage polarization [31, 34]. The mutual exclusivity of STAT-1 and STAT-6 might be a key factor in M1 versus M2 polarization and a potential therapeutic target for HCC aimed at macrophage polarization. In the present study, the addition of LEN increased the level of phosphorylated STAT-1 but had no effect on the level of phosphorylated STAT-6 in macrophages. Fludarabine rescued the effects of LEN on macrophages by inhibiting STAT-1 (Figs. 7 and 8).

In summary, our results suggested that LEN could enhance M1 polarization and inhibit M2 polarization in both humans and mice in vivo. In addition, treatment of macrophages with LEN in vitro could inhibit the proliferation, invasion, and migration of liver cancer cells by promoting M1 macrophage polarization. Finally, STAT-1 was the main target transcription factor of LEN-induced M1 macrophage polarization (Fig. 9). This study provides new evidence for the immunomodulatory activity of LEN in the treatment of hepatocellular carcinoma.

Acknowledgements
Many thanks to Biorender website for their contribution and support to our Graphical Abstract figure.

Author contributions
Peng Sun and Jinming Yu wrote the main manuscript text. Zhenfeng Li, Zaojun Yan and Zhaofeng Wang prepared Figs. 1, 2 and 3. Peng Zheng, Mingliang Wang and Xu Chang prepared Figs. 3 and 4. Zihao Liu and Jianxin Zhang prepared Figs. 5 and 6. Huiyong Wu, Wenbo Shao, Dewen Xue prepared Figs. 7 and 8. All authors reviewed the manuscript.

Funding
This study was supported by Shandong Provincial Natural Science Foundation, China (NO. -ZR2023QH127, ZR2020QH177), the Academic Promotion Program of Shandong First Medical University (2019ZL002), the Research Unit of Radiation Oncology, Chinese Academy of Medical Sciences (2019RU071), the foundation of National Natural Science Foundation of China (81627901, 81972863 and 82030082), the foundation of Natural Science Foundation of Shandong (ZR201911040452).

Data availability
All the data in supportive of this work had been included in the manuscript, and the original raw data was accessible from the corresponding author with reasonable request.

Declarations

Ethics approval and consent to participate
This research was approved by the Medical Ethics Committee of Shandong Cancer Hospital and Institute (SDTHEC2022007011). And the informed consent was obtained from all HCC patients. Animal experimental protocols were approved by the Animal Ethics Committee of Shandong Cancer Hospital and Institute (SDTHEC202201044). All methods involving animals were reported in accordance with ARRIVE (Animal Research: Reporting of In Vivo Experiments) guidelines.

Consent to publish
The authors affirm that human research participants provided informed consent for publication of the images in Fig. 1A and B C.

Competing interests
The authors declare no competing interests.

Received: 14 November 2023 / Accepted: 23 July 2024
Published online: 30 July 2024

References

1. Giraud J, Chalopin D, Blanc JF, Saleh M. Hepatocellular Carcinoma Immune Landscape and the potential of immunotherapies. Front Immunol. 2021;12:655697.
2. Asafo-Agyei KO. H. Samant. Hepatocellular Carcinoma. Treasure Island (FL); 2022.
3. Roxburgh P, Evans TR. Systemic therapy of hepatocellular carcinoma: are we making progress. Adv Ther. 2008;25:1089–104. https://doi.org/10.1007/s12325-008-0113-z.
4. Yarchoan M, Agarwal P, Villanueva A, et al. Recent developments and therapeutic strategies against Hepatocellular Carcinoma. Cancer Res. 2019;79:4326–30. https://doi.org/10.1158/0008-5472.CAN-19-0803.
5. Fu Y, Liu S, Zeng S, Shen H. From bench to bed: the tumor immune microenvironment and current immunotherapeutic strategies for hepatocellular carcinoma. J Exp Clin Cancer Res. 2019;38:396. https://doi.org/10.1186/s13046-019-1396-4.
6. Lewis CE, Pollard JW. Distinct role of macrophages in different tumor microenvironments. Cancer Res. 2006;66:605–12. https://doi.org/10.1158/0008-5472.CAN-05-4005.
7. Jetten N, Verbruggen S, Gijbels MJ, Post MJ, De Winther MP, Donners MM. Anti-inflammatory M2, but not pro-inflammatory M1 macrophages promote angiogenesis in vivo. Angiogenesis. 2014;17:109–18. https://doi.org/10.1007/s10456-013-9381-6.
8. Hume DA. The many alternative faces of macrophage activation. Front Immunol. 2015;6:370. https://doi.org/10.3389/fimmu.2015.00370.
9. Bashir S, Sharma Y, Elahi A, Khan F. Macrophage polarization: the link between inflammation and related diseases. Inflamm Res. 2016;65:1–11. https://doi.org/10.1007/s00011-015-0874-1.
10. Parisi L, Gini E, Baci D, et al. Macrophage polarization in Chronic Inflammatory diseases: killers or builders. J Immunol Res. 2018;2018:8917804. https://doi.org/10.1155/2018/8917804.
11. Fu XT, Song K, Zhou J, et al. Tumor-associated macrophages modulate resistance to oxaliplatin via inducing autophagy in hepatocellular carcinoma. Cancer Cell Int. 2019;19:71. https://doi.org/10.1186/s12935-019-0771-8.
12. Tohyama O, Matsui J, Kodama K, et al. Antitumor activity of lenvatinib (e7080): an angiogenesis inhibitor that targets multiple receptor tyrosine kinases in preclinical human thyroid cancer models. J Thyroid Res. 2014;2014:638747. https://doi.org/10.1155/2014/638747.
13. Yamamoto Y, Matsui J, Matsushima T, et al. Lenvatinib, an angiogenesis inhibitor targeting VEGFR/FGFR, shows broad antitumor activity in human tumor xenograft models associated with microvessel density and pericyte coverage. Vasc Cell. 2014;6:18. https://doi.org/10.1186/2045-824X-6-18.
14. Matsuki M, Hoshi T, Yamamoto Y, et al. Lenvatinib inhibits angiogenesis and tumor fibroblast growth factor signaling pathways in human hepatocellular carcinoma models. Cancer Med. 2018;7:2641–53. https://doi.org/10.1002/cam4.1517.
15. Kimura T, Kato Y, Ozawa Y, et al. Immunomodulatory activity of lenvatinib contributes to antitumor activity in the Hepa1-6 hepatocellular carcinoma model. Cancer Sci. 2018;109:3993–4002. https://doi.org/10.1111/cas.13806.
16. Finn RS, Ikeda M, Zhu AX, et al. Phase ib study of Lenvatinib Plus Pembrolizumab in patients with Unresectable Hepatocellular Carcinoma. J Clin Oncol. 2020;38:2960–70. https://doi.org/10.1200/JCO.20.00808.
17. Zhao Y, Zhang YN, Wang KT, Chen L. Lenvatinib for hepatocellular carcinoma: from preclinical mechanisms to anti-cancer therapy. Biochim Biophys Acta Rev Cancer. 2020;1874:188391. https://doi.org/10.1016/j.bbcan.2020.188391.
18. Ganta VC, Choi M, Farber CR, Annex BH. Antiangiogenic VEGF(165) b regulates macrophage polarization via S100A8/S100A9 in Peripheral Artery Disease. Circulation. 2019;139:226–42. https://doi.org/10.1161/CIRCULATIONAHA.118.034165.
19. Wheeler KC, Jena MK, Pradhan BS, et al. VEGF may contribute to macrophage recruitment and M2 polarization in the decidua. PLoS ONE. 2018;13:e0191040. https://doi.org/10.1371/journal.pone.0191040.
20. Kato Y, Tabata K, Kimura T, et al. Lenvatinib plus anti-PD-1 antibody combination treatment activates CD8 + T cells through reduction of tumor-associated macrophage and activation of the interferon pathway. PLoS ONE. 2019;14:e0212513. https://doi.org/10.1371/journal.pone.0212513.
21. Philip M, Schietinger A. CD8(+) T cell differentiation and dysfunction in cancer. Nat Rev Immunol. 2022;22:209–23. https://doi.org/10.1038/s41577-021-00574-3.
22. Lv R, Bao Q, Li Y. Regulation of M1–type and M2–type macrophage polarization in RAW264.7 cells by Galectin–9. Mol Med Rep. 2017;16:9111–9. https://doi.org/10.3892/mmr.2017.7719.
23. Yang D, Liu A, Wu Y, et al. BCL2L15 depletion inhibits endometrial receptivity via the STAT1 signaling pathway. Genes (Basel). 2020;11. https://doi.org/10.3390/genes11070816.
24. Adachi Y, Kamiyama H, Ichikawa K, et al. Inhibition of FGFR reactivates IFNγ Signaling in Tumor cells to enhance the combined antitumor activity of Lenvatinib with Anti-PD-1 antibodies. Cancer Res. 2022;82:292–306. https://doi.org/10.1158/0008-5472.CAN-20-2426.
25. Gunda V, Gigliotti B, Ashry T, et al. Anti-PD-1/PD-L1 therapy augments lenvatinib's efficacy by favorably altering the immune microenvironment of murine anaplastic thyroid cancer. Int J Cancer. 2019;144:2266–78. https://doi.org/10.1002/ijc.32041.
26. Qian BZ, Pollard JW. Macrophage diversity enhances tumor progression and metastasis. Cell. 2010;141:39–51. https://doi.org/10.1016/j.cell.2010.03.014.
27. Schneider C, Teufel A, Yevsa T, et al. Adaptive immunity suppresses formation and progression of diethylnitrosamine-induced liver cancer. Gut. 2012;61:1733–43. https://doi.org/10.1136/gutjnl-2011-301116.
28. Capece D, Fischietti M, Verzella D, et al. The inflammatory microenvironment in hepatocellular carcinoma: a pivotal role for tumor-associated macrophages. Biomed Res Int. 2013;2013:187204. https://doi.org/10.1155/2013/187204.
29. Kuang DM, Zhao Q, Peng C, et al. Activated monocytes in peritumoral stroma of hepatocellular carcinoma foster immune privilege and disease progression through PD-L1. J Exp Med. 2009;206:1327–37. https://doi.org/10.1084/jem.20082173.
30. Tugal D, Liao X, Jain MK. Transcriptional control of macrophage polarization. Arterioscler Thromb Vasc Biol. 2013;33:1135–44. https://doi.org/10.1161/ATVBAHA.113.301453.
31. Lawrence T, Natoli G. Transcriptional regulation of macrophage polarization: enabling diversity with identity. Nat Rev Immunol. 2011;11:750–61. https://doi.org/10.1038/nri3088.
32. Molawi K, Sieweke MH. Transcriptional control of macrophage identity, self-renewal, and function. Adv Immunol. 2013;120:269–300. https://doi.org/10.1016/B978-0-12-417028-5.00010-7.
33. Ruffell B, Affara NI, Coussens LM. Differential macrophage programming in the tumor microenvironment. Trends Immunol. 2012;33:119–26. https://doi.org/10.1016/j.it.2011.12.001.

34. Li H, Jiang T, Li MQ, Zheng XL, Zhao GJ. Transcriptional regulation of macrophages polarization by MicroRNAs. Front Immunol. 2018;9:1175. https://doi.org/10.3389/fimmu.2018.01175.

Publisher's Note